Characterization of a late transitional B cell population highly sensitive to BAFF-mediated homeostatic proliferation

Almut Meyer-Bahlburg,[1] Sarah F. Andrews,[2] Karl O.A. Yu,[3] Steven A. Porcelli,[3] and David J. Rawlings[1,2]

[1]Department of Pediatrics and [2]Department of Immunology, University of Washington School of Medicine, Seattle, WA 98195
[3]Department of Microbiology and Immunology, Albert Einstein College of Medicine Bronx, NY 10461

We have characterized a distinct, late transitional B cell subset, CD21^{int} transitional 2 (T2) B cells. In contrast to early transitional B cells, CD21^{int} T2 B cells exhibit augmented responses to a range of potential microenvironmental stimuli. Adoptive transfer studies demonstrate that this subset is an immediate precursor of both follicular mature and marginal zone (MZ) B cells. In vivo, a large percentage of CD21^{int} T2 B cells has entered the cell cycle, and the cycling subpopulation exhibits further augmentation in mitogenic responses and B cell–activating factor of the TNF family (BAFF) receptor expression. Consistent with these features, CD21^{int} T2 cells exhibit preferential responses to BAFF-facilitated homeostatic signals in vivo. In addition, we demonstrate that M167 B cell receptor (BCR) idiotypic-specific B cells are first selected within the cycling CD21^{int} T2 population, ultimately leading to preferential enrichment of these cells within the MZ B cell compartment. These data, in association with the coordinate role for BAFF and microenvironmental cues in determining the mature BCR repertoire, imply that this subset functions as a unique selection point in peripheral B cell development.

CORRESPONDENCE
David J. Rawlings:
drawling@u.washington.edu

Abbreviations used: AAD, amino actinomycin D; BAFF, B cell-activating factor of the TNF family; BAFF-R, BAFF receptor; BCR, B cell receptor; FM, follicular mature; HP, homeostatic proliferation; KREC, κ-deleting recombination excision circle; MZ, marginal zone; MZP, MZ precursor; PC, phosphorylcholine; TLR, Toll-like receptor.

Postfetal B cell development initiates in the BM from a common lymphoid progenitor and progresses via sequential developmental stages to generate immature B cells that express a functional B cell receptor (BCR). Immature B cells subsequently migrate through the bloodstream to the spleen, where progression through "transitional" developmental stages is required to form naive mature B cells capable of differentiating into antibody-secreting cells upon encounter with cognate antigen (1).

Developing B cells are first tested for self-tolerance in the BM after expression of the newly arranged BCR on the cell surface. Cells that encounter self-antigen are either deleted, undergo receptor editing, or become anergic, depending on the affinity and the physical form of the antigen encountered (2, 3). Despite these events, a significant number of newly formed, self-reactive B cells survive to enter the periphery, suggesting that additional tolerance checkpoints must operate during splenic transitional B cell development. In humans, the relative number of self-reactive B cells decreases from ∼40 to 20% as newly formed immature B cells transition into the naive mature B cell compartment (4). This progressive decline in self-reactive cells fails to occur in patients with systemic lupus erythematosus or rheumatoid arthritis, supporting the conclusion that peripheral selection is essential for maintaining B cell self-tolerance (5, 6). Consistent with these observations, transgenic studies have also shown that if self-antigen expression is limited to the periphery, tolerance of self-reactive mouse B cells occurs primarily within the transitional compartment (7, 8).

In addition to negative selection, several lines of evidence suggest that positive selection may also play an important role in shaping the naive mature B cell repertoire. Studies comparing the BCR repertoire in BM versus peripheral B cells have shown differences in V-gene usage and a bias toward specific light chain/heavy chain combinations, suggesting selection for certain BCRs (9, 10). In circumstances where self-antigen is expressed at very low levels or in which BCR signaling is reduced, B cells that recognize self-antigen can exhibit a selective

A. Meyer-Bahlburg and S.F. Andrews contributed equally to this paper.
The online version of this article contains supplemental material.

advantage (11, 12). Similarly, transgenic B cell development arrests at the transitional B cell stage in the absence of ligand, and can be rescued either by BCR stimulation or adoptive cell transfer into lymphopenic hosts that express the relevant cognate self-antigen (13). Finally, antigen selection is also evident within the marginal zone (MZ) compartment, where self-reactive transgenic B cells are specifically enriched within the mature MZ B cell population (14).

Although BCR specificity is important in determining whether an individual B cell survives the transitional "bottleneck," responses to key environmental signals also significantly contribute to determining B cell fate. In particular, B cell–activating factor of the TNF family (BAFF) appears to play a critical role in peripheral B cell tolerance. This prosurvival cytokine is necessary for B cell survival and differentiation beyond the late transitional stage, which is when BAFF receptor (BAFF-R) surface expression reaches a threshold level (15, 16). Competition for limiting levels of BAFF has been hypothesized to favor self-tolerant B cells during peripheral B cell development (17, 18). Consistent with this idea, BAFF overexpression expands both the late transitional and mature peripheral B cell compartments and promotes B cell–mediated autoimmunity, in part, through enhanced survival of low-affinity self-reactive B cells.

Despite mounting evidence that environmental cues significantly impact the mature BCR repertoire, studies to date have failed to identify a transitional subset capable of competitive expansion in response to such signals. In this study, we have sought to directly address this issue. We have characterized a bipotent, nonquiescent, phenotypically and functionally distinct, late transitional B cell subset that is uniquely sensitive to mitogenic and homeostatic signals. Further, our data indicate that self-reactive B cells within this subset can be selectively expanded. Our combined findings indicate that these transitional precursors function as a sensitive cellular pool capable of responding to changing environmental stimuli, and can thereby operate as a key checkpoint in peripheral B cell tolerance.

RESULTS

CD21^{int} transitional 2 (T2) B cells comprise a distinct B cell subset

The precise sequence of differentiation of late splenic transitional B cells remains incompletely defined. Investigation from our own and other laboratories has suggested that the T2 B cell subset (CD21$^{hi/int}$IgM^{hi}IgD^{hi}CD24^{hi}) as originally defined by Loder et al. (19) represents a heterogeneous population. Pillai first introduced the idea of further delineating this population based on the relative expression of CD21 into T2-follicular precursor (CD21^{int}) and T2-MZ precursor (T2-MZP; CD21^{hi}) subsets (20). Although the properties of CD21^{hi} T2 B cells have become relatively well defined (20–22), little experimental data exists in regard to the functional properties and potential developmental capacity of CD21^{int} transitional B cells. We therefore initiated studies to define the properties of this B cell subpopulation in greater detail.

As shown in Fig. 1 A, CD24^{hi} B cells can be subdivided by CD21 expression into CD21^{lo} (which are labeled T1 B cells according to the Loder classification [19]), CD21^{int} (henceforth labeled CD21^{int} T2 B cells), and CD21^{hi} B cells. CD21^{lo} T1 B cells can be further divided into CD23^{lo} and CD23^{hi} subsets (which largely correspond to the T1 and T2 subsets described by Allman et al. [23]) and are hereafter referred to as CD23^{lo} T1 and CD23^{hi} T1 B cells. CD21^{int} cells are largely CD23^{hi}, whereas CD21^{hi} cells contain CD23^{hi} T2-MZP and CD23^{lo} MZ B cells. Follicular mature (FM) B cells express intermediate levels of both CD24 and CD21. The CD21^{int} T2 cells comprise 1–2% of total splenocytes from 8–12-wk-old mice (Fig. 1 B), and using 8-color flow cytometry we determined that they express high levels of IgM, IgD, AA4.1, CD23, and CD62L and intermediate-to-low levels of LFA-1 and CD1d (Fig. 1 C and Table S1, available at http://www.jem.org/cgi/content/full/jem.20071088/DC1). These combined phenotypic features are consistent with classification as a late transitional population. As an alternative measure of cell maturity, we evaluated relative GFP expression in Rag2p-GFP transgenic mice (24). In this model, Rag2 expression terminates at the immature BM B cell stage and GFP expression within the spleen is restricted to newly formed immature B cells (25). Analysis of GFP expression indicated that CD21^{int} T2 B cells, like T1 cells, express high levels of GFP in contrast to the GFP$^-$ T2-MZP, MZ, and FM B cells (Fig. 1 D). Interestingly, a small percentage of CD21^{int} T2 B cells were GFP$^-$; the significance of this finding will be discussed in detail below.

Notch signaling has been shown to play a crucial role in the development of T2-MZP and MZ B cells (21). To further delineate CD21^{int} T2 B cells from CD21^{hi} T2-MZP and MZ B cells, we determined relative expression of the Notch target genes *hes1* and *deltex1*. As previously shown (21), Hes1 and Deltex1 expression was increased three- to fivefold in T2-MZP and MZ relative to T1, CD21^{int} T2, or FM B cells (Fig. 1 E). In addition, Notch2 haplodeficient mice exhibited no reduction in CD21^{int} T2 B cells, whereas T2-MZP and MZ numbers were reduced by 40–60% (unpublished data), indicating that Notch signaling is not essential for CD21^{int} T2 B cell development.

We next determined the in vitro functional responses of CD21^{int} T2 B cells to Toll-like receptor (TLR) or BCR ligation (Fig. 2 A). CD21^{int} T2 B cells proliferated robustly in response to LPS stimulation, similar to T2-MZP or MZ B cells. This response was significantly greater than in either T1 or FM B cells. BCR engagement led to a partial proliferative response in CD21^{int} T2 B cells, in contrast to T1 B cells. To further characterize this response, sorted cells were labeled with CFSE and cell division and survival were evaluated. After 48 h, although only a limited number of CD21^{int} T2 B cells survived, this population exhibited a rate of cell division that paralleled the response of FM B cells (Fig. 2 B). In contrast, no T1 cells survived BCR cross-linking. To exclude contamination with FM as the source of proliferating cells within CD21^{int} T2 cells, we performed parallel assays using mixtures of 90–95% T1 and 5–10% FM B cells (to mimic the maximal level of FM

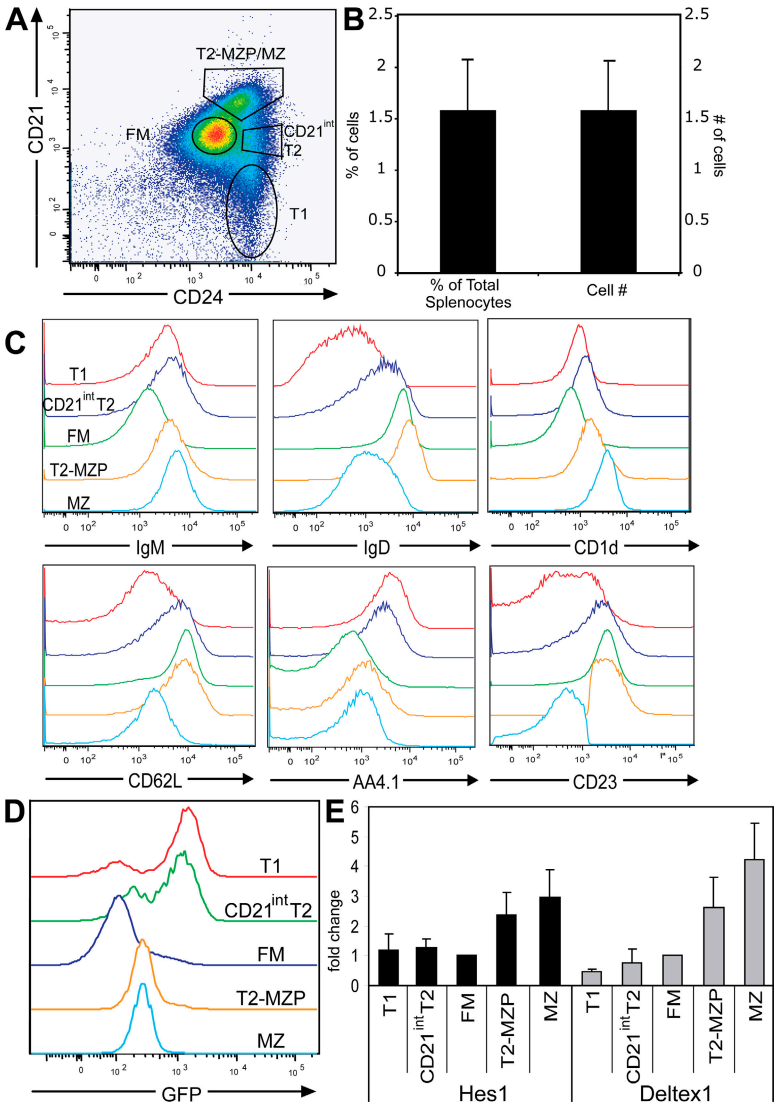

Figure 1. Characterization of CD21^{int} T2 B cells. (A–C) Expression of surface markers on splenic B cell subsets. (A) B220^{+}/CD19^{+} splenic B cell subsets gated based on CD21 and CD24. (B) Percentage and absolute number of CD21^{int}T2 cells within total splenic lymphocytes in 8–12-wk-old C57BL/6 mice (mean of 3 independent experiments). (C) Expression of IgM, IgD, CD62L, AA4.1, CD23, and CD1d in splenic B cell subsets. Representative of more than five independent experiments. (D) GFP expression in splenic B cell subsets from an 8-wk-old Rag2p-GFP transgenic mouse. (E) Expression of Notch target genes. Relative Hes1 and Deltex1 expression are shown as fold change of each subset relative to FM B cells set as 1. Data represented as the mean with SD from four independent experiments.

potentially present within the sorted CD21^{int} T2 population; Fig. S1, available at http://www.jem.org/cgi/content/full/jem.20071088/DC1) and observed no proliferation (Fig. 2 B).

To directly evaluate proapoptotic signaling, we measured BCR-induced activation of caspase 3. Although T1 cells exhibited a rapid increase in active caspase 3, this response was markedly blunted in CD21^{int} T2 B cells, similar to that in FM B cells. This reduction in caspase activity correlated with increased survival relative to T1 B cells with and without BCR engagement (Fig. 2, C and D).

In summary, CD21^{int} T2 B cells represent a phenotypically and functionally distinct transitional population. High expression of GFP, AA4.1, and CD24 clearly characterize CD21^{int} T2 B cells as immature splenic B cells. They are distinct from T1 B cells based on IgD, CD62L, and LFA-1 expression; increased resistance to BCR-induced cell death; and robust proliferation to TLR signaling. Finally, in contrast to CD24^{hi}CD21^{hi} T2-MZP and MZ B cells, CD21^{int} T2 B cells exhibit no evidence for increased Notch signals.

CD21^{int} T2 B cells develop after T1 B cells

The slightly lower expression of both GFP and AA4.1 in CD21^{int} T2 versus T1 B cells suggested that CD21^{int} T2 B cells were derived from T1 cells. To test this idea, we evaluated peripheral B cell reconstitution after sublethal irradiation. Adult C57BL/6 mice were irradiated with 500 cGy and

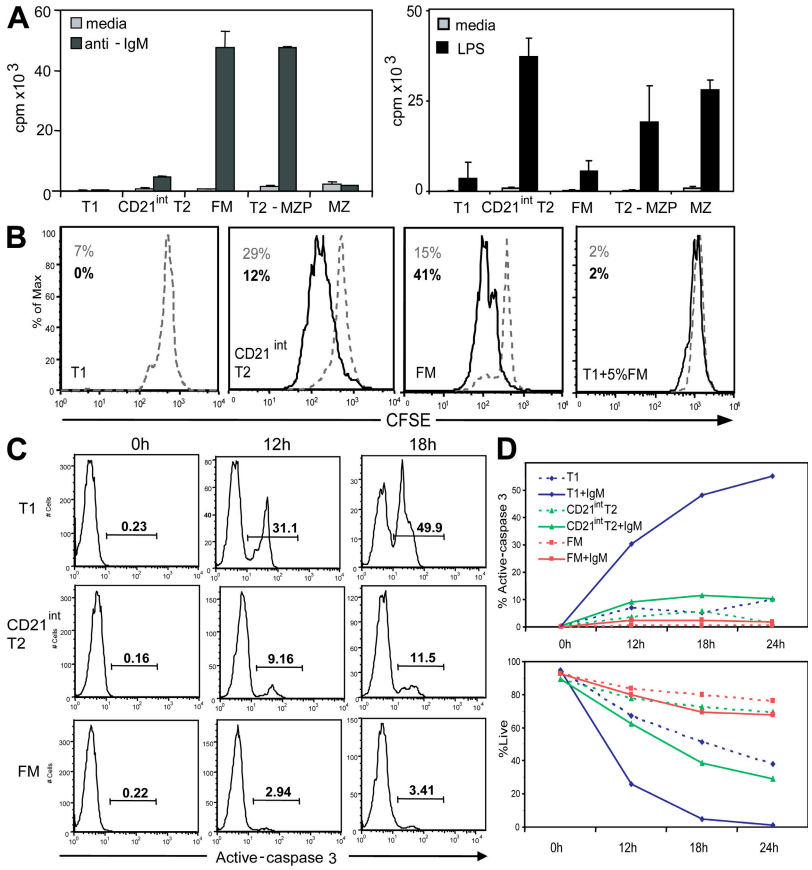

Figure 2. CD21^{int} T2 B cells are functionally distinct. (A) Proliferative responses of purified B cell subsets after incubation for 48 h in media alone, with anti-IgM or LPS. (B) CFSE-labeled B cell subsets were cultured in media alone (dashed lines) or with anti-IgM (solid lines) for 48 h, and proliferation was analyzed by dilution of CFSE. Numbers indicate the percentage of live cells in unstimulated versus anti-IgM–stimulated (bold) cultures. T1 cells did not survive anti-IgM stimulation, so no trace is shown. (C) Sorted cells were cultured with anti-IgM and apoptosis measured by caspase 3 activity at indicated time points. Numbers indicate the percentage of active caspase 3$^+$ cells within the live lymphocyte gate. (D) Kinetic analysis of caspase 3 activity and cell survival. (top) The percentage of active caspase 3$^+$ cells from the experiment shown in C. (bottom) The percentage of live cells, based on 7-AAD staining over time with or without BCR engagement. Data are representative of at least three independent experiments.

splenocytes analyzed on day 11, 13, 15, 17, and 19 after irradiation (Fig. 3). Whereas T1 B cells peaked on day 13, the number of CD21^{int} T2 B cells was maximal on day 15–17 and decreased markedly by day 19. In contrast, the number of FM B cells progressively increased between day 13 and 17, and they comprised the majority of cells by day 17–19. Smaller numbers of CD21^{hi} T2-MZP and MZ B cells could be identified beginning at day 17. A similar progression in B cell subset development was seen via analysis of splenic B cell subsets in unmanipulated neonates at various ages (unpublished data).

CD21^{int} T2 B cells comprise a bipotent precursor for FM and MZ B cells

To directly analyze the developmental capacity of CD21^{int} T2 B cells, we performed adoptive cell transfer experiments. To obtain sufficient numbers of this relatively rare population, CD24^{hi}CD21^{int}IgM^{hi} B cells were purified from sublethally irradiated mice (day 15). Postsort purities were consistently >90%, with <0.2% contaminating T2-MZP/MZ and <1.5% FM B cells. Though more contaminating T1 cells were present, these should not alter our experimental interpretation, as they comprise precursors for CD21^{int} T2 B cells. Sorted populations exhibited the features of CD21^{int} T2 cells based on phenotypic markers, relative Deltex1 and Cyclin D2 mRNA expression, and BCR and TLR responses (Fig. S2, A-E, available at http://www.jem.org/cgi/content/full/jem.20071088/DC1).

Purified Ly5.1$^+$ CD21^{int} T2 B cells were labeled with CFSE and injected into nonlymphopenic, adult Ly5.2$^+$ C57BL/6 mice. Similar to previously published results (22), recovery of transferred cells was 1–1.5%. Even as early as day 1, transferred CD21^{int} T2 B cells developed into both FM (CD24^{int}CD21^{int}IgM^{lo}CD1d^{lo}) and T2-MZP/MZ (CD24^{hi}CD21^{hi}IgM^{hi}CD1d^{hi}) B cells (Fig. 4). We conclude from these data that the CD21^{int} T2 subset contains immediate precursors for both FM and T2-MZP/MZ B cells.

CD21^{int} T2 B cells cycle in vivo

We observed a significant number of larger cells within the CD21^{int} T2 cell population in contrast to either T1 or FM B cells (Fig. S3 A, available at http://www.jem.org/cgi/content/

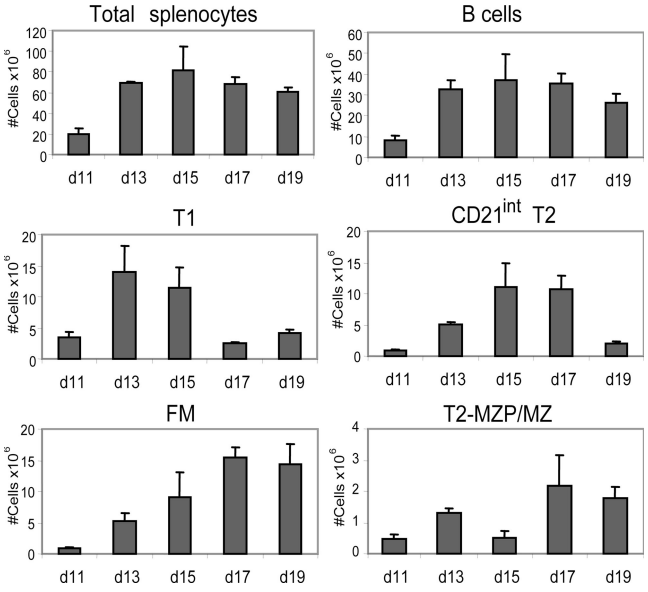

Figure 3. CD21^{int} T2 B cells develop after T1 B cells. Kinetic analysis of splenic B cell reconstitution after sublethal irradiation. C57BL/6 mice were irradiated with 500 cGy, and splenocytes were analyzed at the indicated time points. Shown is the mean of absolute numbers of each B cell subset with SD from three animals. Representative of three independent experiments.

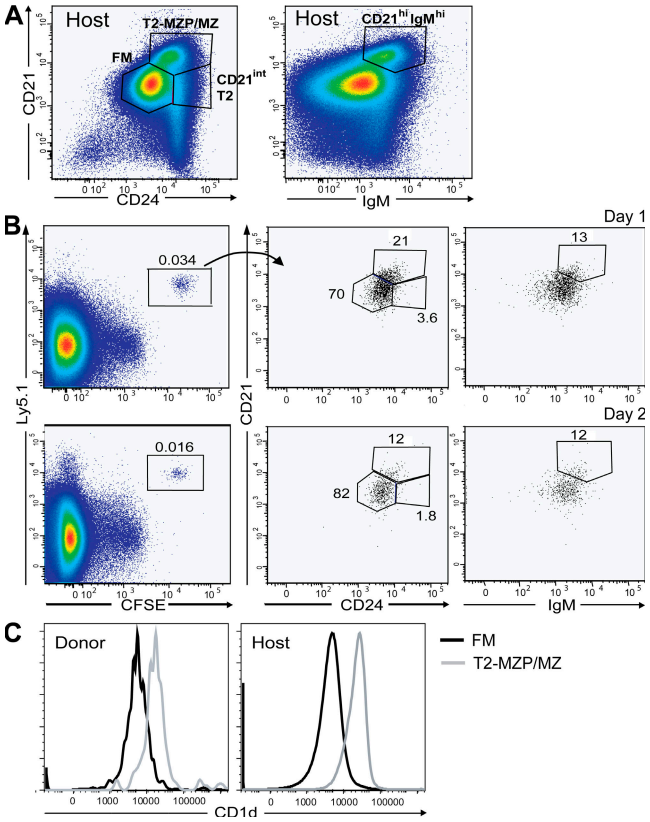

Figure 4. CD21^{int} T2 B cells contain precursors for both FM and T2-MZP/MZ B cells. CD21^{int} T2 B cells were purified from sublethally irradiated mice, labeled with CFSE, and 1–2 × 10^6 cells/recipient were transferred into Ly5.2$^+$ C57BL/6 mice. Recipient animals were killed at day 1 or 2 after transfer, and splenocytes were analyzed by staining with the indicated markers. (A) After initial gating of host B220$^+$CD19$^+$ B cells, splenic B cell subsets were identified as in Fig. 1 (left); and T2-MZP/MZ were additionally characterized as IgM^{hi}CD21^{hi} cells (right). (B, left) Donor cells identified as Ly5.1$^+$CFSE$^+$. (middle and right) Donor B cell subsets determined based on gating shown in A. (C) Donor and recipient FM and T2-MZP/MZ B cells were compared for relative expression of CD1d. Data shown are representative of three experiments with two mice per day for each experiment.

full/jem.20071088/DC1), suggesting that they were more activated. To address this possibility, we stained splenic B cell populations immediately ex vivo using Pyronin Y and DAPI to measure RNA and DNA content, respectively, thereby allowing us to determine the percentage of cells in each phase of the cell cycle (Fig. S3 B) (26). Cell doublets were carefully excluded before cell-cycle analysis based on DAPI width and area. Although on average, >85% of T1 and FM B cells were in G0, ∼50% of CD21^{int} T2 cells were in G1, and ∼5% of CD21^{int} T2 cells had further progressed into S and G2 phases (Fig. 5 A).

These data strongly suggested that splenic CD21^{int} T2 cells were proliferating in vivo. To directly test this idea, we performed in vivo BrdU-labeling experiments. We tested the prediction that, at early time points, BrdU incorporation would be significantly higher in CD21^{int} T2 cells compared with T1 B cells. At later times, we also predicted that (after the influx of newly formed BrdU-labeled cells from the BM), a larger percentage of T1 B cells would be BrdU$^+$, as this population would comprise the precursors for additional CD21^{int} T2 B cells. Animals were fed BrdU continuously via the drinking water, and BrdU incorporation was analyzed within each splenic B cell subset at the indicated time points. On day 1 and 2 after BrdU administration, a significantly higher percentage of CD21^{int} T2 cells was BrdU$^+$ (Fig. 5, B and C). However, this ratio reversed on day 4 and 5, with more T1 B cells labeled with BrdU. Consistent with previous results (23), BrdU labeling was higher in CD23^{lo} compared with CD23^{hi} T1 cells (Fig. 5 D).

We compared the functional activity and phenotype of quiescent versus active (G1, S, or G2) CD21^{int} T2 cells. Although the majority of transgenic CD21^{int} T2 B cells were GFP$^+$, a limited subpopulation was GFP$^-$ (∼25–35%; Fig. 1 D). As GFP is no longer transcribed, cell division was anticipated to dilute out the GFP signal in this subset. Thus, we evaluated the percentage of GFP$^+$ versus GFP$^-$ CD21^{int} T2 cells that had progressed beyond G0, and we observed an approximately twofold increase within the GFP$^-$ subset (Fig. 6, A and B). The surface phenotype of resting versus cycling cells, however, remained indistinguishable, indicating that these populations represented nearly identical stages in development (Fig. S4, available at http://www.jem.org/cgi/content/full/jem.20071088/DC1). Strikingly, GFP$^-$ CD21^{int} T2 B cells exhibited a significant enhancement in their response to BCR engagement, mainly through increased survival, yet retained

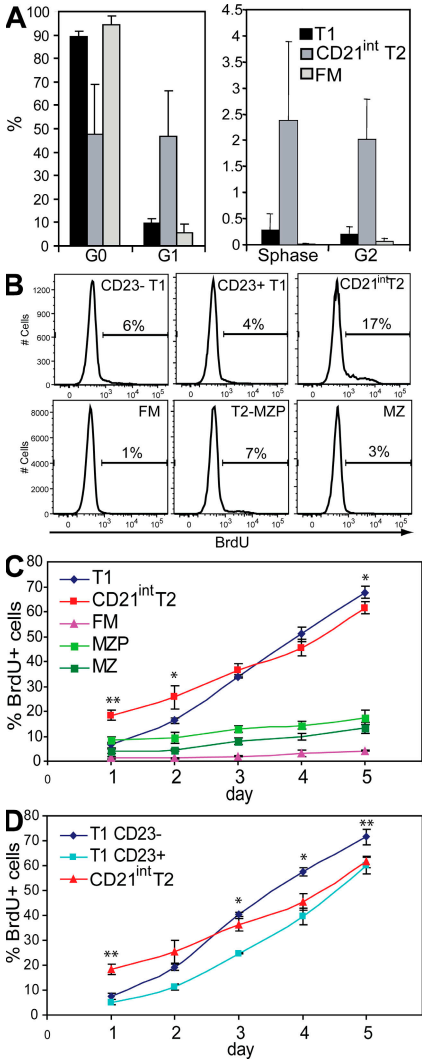

Figure 5. CD21^{int} T2 B cells cycle in vivo. (A) Cell cycle analysis. Total splenocytes from BALB/c mice were stained for B220, IgM, CD21, and CD24, and then fixed and stained with DAPI and Pyronin Y. After doublet exclusion, B220^{+} cells were identified as T1, CD21^{int} T2, or FM B cells, and the percentage of cells within each phase of cell cycle was determined. Data are shown as the mean with SD of five independent experiments. (B–D) BrdU labeling of splenic B cell subsets. (B) Representative FACS histogram of BrdU labeling in splenic B cells 1 d after continuous BrdU administration. (C and D) Percentage of BrdU^{+} cells in splenic B cell subsets (C) and CD23^{lo} versus CD23^{hi} T1 and CD21^{int} T2 B cells (D) over time after continuous BrdU administration. *, $P < 0.05$; **, $P < 0.01$ for CD21^{int} T2 compared with T1 or CD23^{lo} T1 cells. Data are representative of two independent experiments, and the mean with SD of three mice per time point is shown.

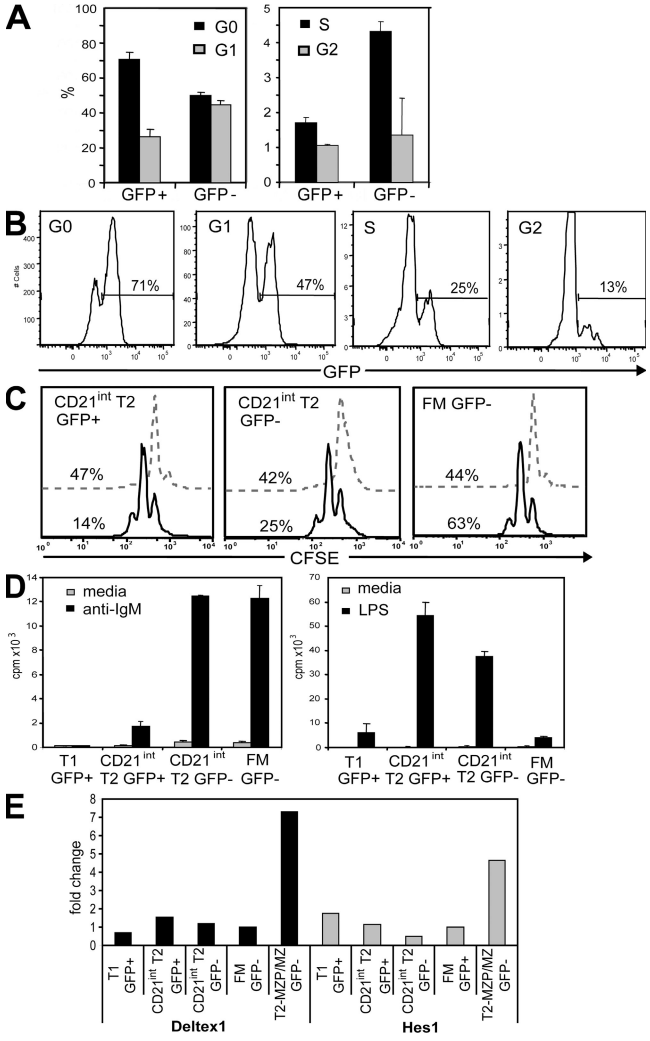

Figure 6. Cycling CD21^{int} T2 B cells are GFP^{-}. (A) Cell cycle status of GFP^{+} versus GFP^{-} CD21^{int} T2 B cells. Data are the mean with SD from three independent experiments showing the percentage of CD21^{int} T2 B cells within each phase of the cell cycle. (B) GFP expression in CD21^{int} T2 B cells at distinct phases of cell cycle. CD21^{int} T2 B cells from Rag2p-GFP Tg mice were identified, and relative GFP expression was determined for each phase of the cell cycle. (C) CFSE dilution of GFP^{+} versus GFP^{-} CD21^{int} T2 cells in response to BCR engagement. CFSE-labeled CD21^{int} T2 B cells were cultured in media alone (dashed lines) or anti-IgM (black lines) for 48 h, and proliferation was determined by dilution of CFSE. Numbers shown indicate the percentage of live cells under each condition. (D) Mitogenic responses of GFP^{+} versus GFP^{-} CD21^{int} T2 B cells. Sorted splenic B cell subsets were cultured in media alone, with anti-IgM, or with LPS, and proliferation was determined. (E) Expression of Notch target genes. Splenic B cell subsets were sorted from Rag2p-GFP Tg mice, and the transcript levels of Deltex1 and Hes1 was determined. Displayed as fold change in expression relative to FM B cells set as 1. All data shown are representative of at least three separate experiments.

the strong proliferative response to TLR signals (Fig. 6, C and D). Although the mitogenic responses of GFP^{-} CD21^{int} T2 cells were nearly identical to that observed for T2-MZP B cells (Fig. 2 A) (27), this subset exhibited no evidence of increased Notch2 signaling (Fig. 6 E).

A recent study has used κ-deleting recombination excision circles (KRECs), which are generated during light chain rearrangement, to determine the in vivo replication history of B cells (28). Therefore, we used this method to independently verify that GFP^{-} CD21^{int} T2 B cells have undergone

cell divisions in vivo. The ΔC_T between genomic coding joints and the signal joint of KRECs (equivalent to the number of cell divisions) in GFP$^-$ CD21^{int} T2 cells was comparable to T2-MZP/MZ cells, which were previously shown to have undergone several cell divisions (Fig. 7 A) (28). In contrast, T1, FM, or GFP$^+$ CD21^{int} T2 B cells had undergone only 1–2 cell divisions.

CD21^{int} T2 B cells cycle preferentially in response to homeostatic signals

Although one key characteristic of CD21^{int} T2 B cells was their capacity to proliferate in vivo, it remained unclear which environmental factors influence proliferation. In our transfer experiments using nonlymphopenic hosts, we observed minimal proliferation for up to 7 d after transfer (unpublished data). This finding was in accordance with published data, indicating that lymphopenia is the major stimulus for B cell homeostatic proliferation (HP) (29). Thus, we used recipient B cell–deficient μMT mice to compare the capacity of different B cell subsets to respond to signals inducing HP.

Purified Ly5.1$^+$ T1 cells were labeled with CFSE and transferred into unmanipulated μMT mice (Ly5.2$^+$) along with "feeder" B cells to partially blunt homeostatic signals (30). Splenocytes were isolated on day 2, 4, or 7 after transfer and evaluated for surface phenotype and relative proliferation by dilution of CFSE (Fig. 8 A). Among recovered splenic B cells, 1.5–2.5% were Ly5.1$^+$ (derived from transferred T1 cells). The percentage of T1 cells at each of these time points was negligible (<0.5%), and, accordingly, this subset is not shown in the data presented. Within 2 d, ∼7% of labeled B cells had proliferated, and this proportion increased progressively to 62% by day 7. Consistent with this kinetic, CD21^{int} T2 cells had begun to proliferate at day 2, and nearly all cells within this gate proliferated within 7 d. We also identified transferred cells with a T2-MZP/MZ or FM B cell phenotype that had proliferated, albeit at a much lower percentage. These observations indicate that CD21^{int} T2 B cells preferentially cycle in a lymphopenic environment.

Next, we transferred purified, CFSE-labeled, Ly5.1$^+$ CD21^{int} T2 B cells (sorted from sublethally irradiated mice) into Ly5.2$^+$ μMT mice together with "feeder" B cells to directly assess the CD21^{int} T2 B cell response to homeostatic signals. Transferred cells markedly proliferated, with 55% having divided by day 3, and ∼65% having divided by day 5 and 7 after transfer (Fig. 8 B). Similar to transfer experiments in B cell–sufficient hosts, CD21^{int} T2 B cells developed into both FM and T2-MZP/MZ B cells. Analysis of various subsets demonstrated that CD21^{int} T2 B cells proliferated to the greatest extent, followed by T2-MZP/MZ cells, suggesting that CD21^{int} T2 B cell proliferation precedes that within the MZ pool. In contrast, newly formed FM B cells exhibited minimal proliferation. Transferred CD21^{int} T2 B cells also proliferated at earlier time points in comparison to cells derived from T1 B cells (Fig. 8, A and B), suggesting a requirement for T1 cell differentiation before active proliferation.

We also transferred GFP$^-$ FM B cells from Rag2p-GFP transgenic mice into μMT mice to determine whether FM B cells might give rise to proliferating cells with a CD21^{int} T2 cell phenotype. Transferred FM B cells proliferated (30–40% on day 7 after transfer), albeit significantly less extensively than transferred CD21^{int} T2 B cells (Fig. 8, B and C). However, although we clearly identified T2-MZP/MZ B cells (∼60–80%) derived from the input FM population, no donor cells acquired a CD21^{int} T2 B cell phenotype (<1%). Thus, although FM B cells can cycle in response to homeostatic signals, cycling CD21^{int} T2 B cells are generated at an earlier developmental stage. These findings indicate that GFP$^-$ CD21^{int} T2 cells are not derived from FM B cells, which is consistent with our interpretation that GFP$^+$ and GFP$^-$ CD21^{int} T2 cells represent closely related precursors of mature B cells.

Collectively, these results indicate that the CD21^{int} T2 B cell subset is poised to respond to homeostatic signals. However, although proliferation could accompany differentiation, it is not required for generation of the mature B cell pool. These additional transfer studies also support the hypothesis that CD21^{int} T2 B cells develop from T1 B cells, and subsequently give rise to both FM and T2-MZP/MZ B cells.

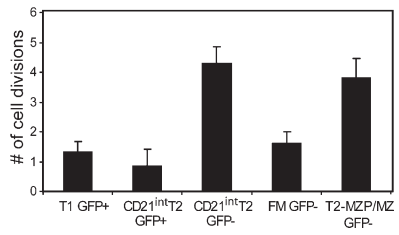

Figure 7. GFP$^-$ CD21^{int}T2 have undergone several cell divisions. B cell subsets were sorted from Rag2p-GFP transgenic mice. The number of cell divisions, based on the ΔC_T between the coding joint of rearranged genomic DNA and signal joint of KRECs formed during IRS-to-RS rearrangement in the κ-chain locus was determined by real-time PCR. Mean with SD from two independent experiments.

BAFF inhibition limits B cell HP

We next sought to identify stimuli that could induce HP of CD21^{int} T2 B cells. Among candidate growth factors, available data strongly implicate BAFF in splenic B cell survival and homeostasis (31, 32). Recent data also indicate that B cell deficiency leads to elevated plasma levels of BAFF (18). We therefore determined whether partial blocking of BAFF in B cell–deficient mice would alter the proliferative response of CD21^{int} T2 B cells.

To test this idea, we used an adenovirus vector encoding for TACI-Fc (TACI-Ad), which was previously demonstrated to block BAFF activity in vivo (33). Recipient μMT mice were injected i.v. with TACI-Ad or a control GFP vector, GFP-Ad. 7 d later, we adoptively transferred CFSE-labeled splenic B cells, and proliferation of transferred cells was analyzed at day 5 after transfer (Fig. 9 A). B cells in TACI-Ad–infected recipients exhibited lower expression of CD21, which is a direct target of BAFF signaling (34), and reduced numbers of CD21^{hi}CD1d^{hi} T2-MZP/MZ B cells (Fig. S5, available at

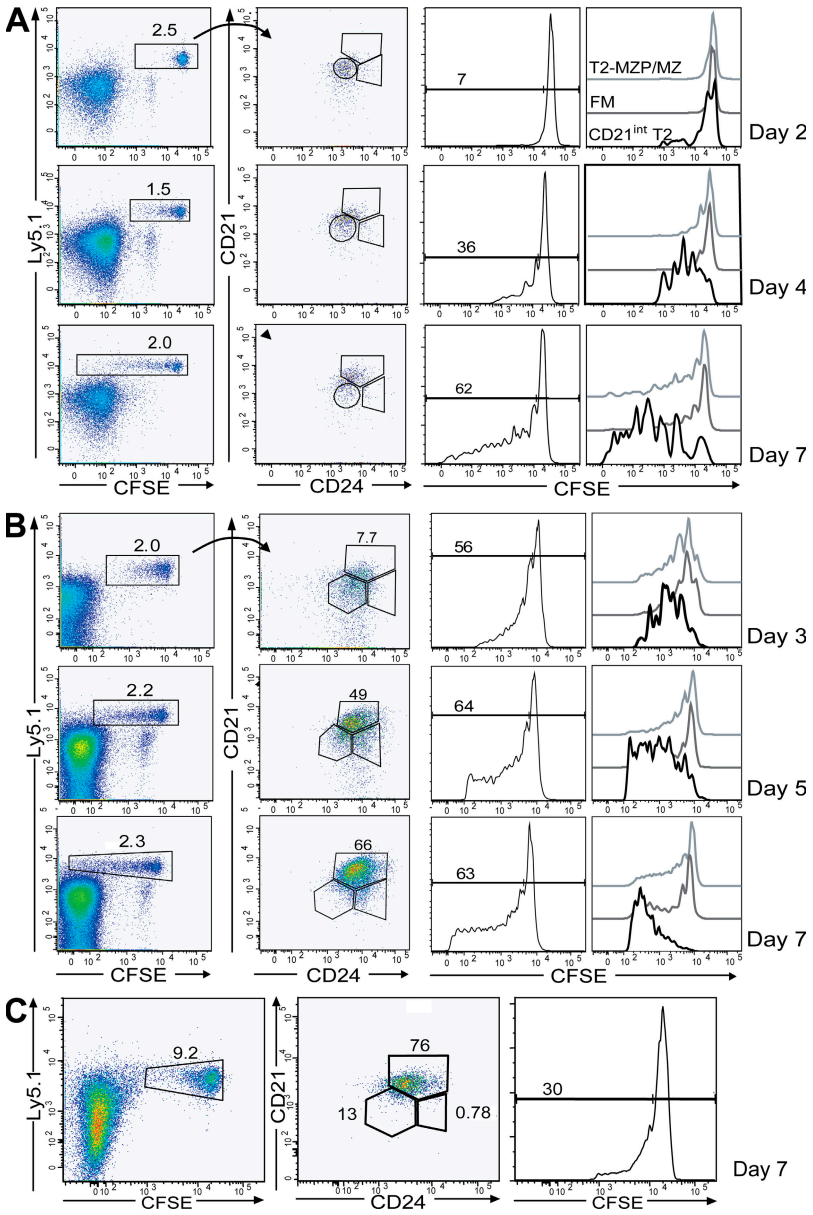

Figure 8. CD21^{int} T2 B cells cycle preferentially in response to homeostatic signals. (A–C) Transfer of T1, CD21^{int} T2, or FM B cells into μMT mice. 1–2 × 10^6 purified Ly5.1$^+$ T1 B cells (A), CD21^{int} T2 B cells from irradiated mice (B), or GFP$^-$ FM B cells (C) were labeled with CFSE and transferred into μMT mice together with feeder B cells (13–14 × 10^6 unlabeled CD43$^-$Ly5.2$^+$ splenic B cells/recipient). Recipients were killed on indicated days after transfer, and splenocytes were stained as indicated. Gates were set according to cells from a control C57BL/6 mouse. (first column) Gated analysis of B220$^+$CD19$^+$ B showing Ly5.1$^+$CFSE$^+$ donor cells. (second column) Analysis of Ly5.1$^+$CFSE$^+$ B cell subsets. (third column) CFSE dilution in transferred Ly5.1$^+$ B cells. (fourth column; A and B only) CFSE dilution within each Ly5.1$^+$ B cell subset. Data from one of two (A and C) or three (B) independent experiments (with two mice per time point) are shown.

http://www.jem.org/cgi/content/full/jem.20071088/DC1). BAFF inhibition also significantly reduced the number of proliferating B cells (Fig. 9 A), which is consistent with unpublished observations cited in a recent review (30). Most notably, a detailed subset analysis clearly indicated the preferential loss of proliferative responses within the CD21^{int} T2 population.

The reduction in HP after BAFF inhibition suggested that preferential cycling of CD21^{int} T2 B cells in vivo might reflect a greater capacity to compete for available BAFF. To address this idea, we analyzed BAFF-R expression in CD21^{int} T2 versus other B cell subsets; and, specifically, within cycling versus noncycling CD21^{int} T2 B cells. Bulk CD21^{int} T2 cells had higher BAFF-R levels than either T1 or FM B cells. Strikingly, GFP$^-$ CD21^{int} T2 cells expressed the highest BAFF-R levels among all subsets (Fig. 9 B). Further, relative BAFF-R expression was greater in CD21^{int} T2 B cells in G1-G2 versus

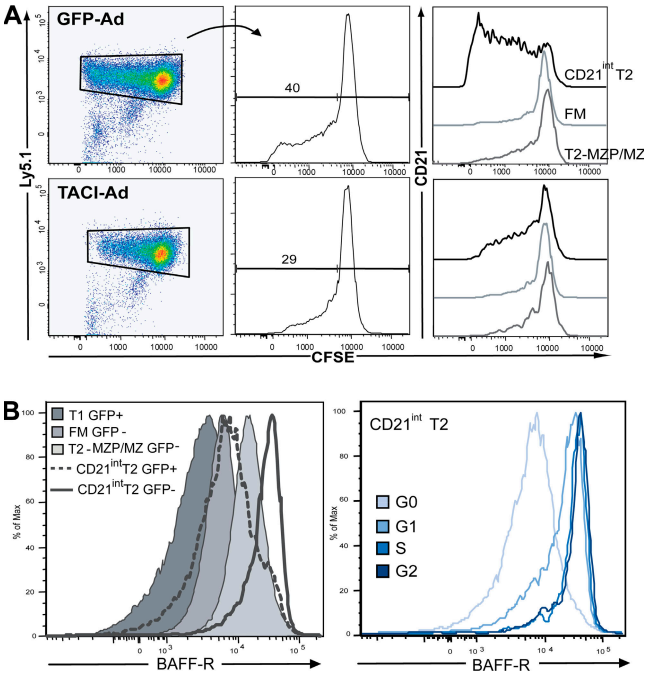

Figure 9. BAFF signals contribute to CD21^{int} T2 B cell HP. (A) Effect of BAFF inhibition on HP. μMT mice were treated with TACI- or control GFP-adenovirus 7 d before transfer of CFSE-labeled splenic B cells (20×10^6 CD43$^-$ Ly5.1$^+$ cells/recipient). Mice were killed 5 d after transfer, and splenocytes were surface stained. Ly5.1$^+$ transferred cells (left) were analyzed for dilution of CFSE (right). (B) BAFF-R expression. Total splenic B cells from Rag2p-GFP Tg mice were stained for B220, IgM, CD24, and CD21 and BAFF-R, and BAFF-R expression was compared between B cell subsets (left) or in CD21^{int} T2 cells at each phase of cell cycle (right). Representative of more than five experiments.

those in G0. This difference was not secondary to cell size, as expression of other surface markers remained unaltered (unpublished data).

Collectively, these results indicate that CD21^{int} T2 B cells preferentially cycle in response to homeostatic stimuli, and imply that this differential sensitivity is controlled by an enhanced capacity to respond to BAFF.

Cycling CD21^{int} T2 B cells show evidence of antigen-driven expansion

To look specifically for evidence of antigen-driven expansion of CD21^{int} T2 B cells, we first determined the relative κ- versus λ-light chain usage among peripheral B cell subsets. The majority of immature B cells express a BCR containing a κ-light chain as opposed to an λ-light chain, and the relative fraction of λ$^+$ B cells declines between the immature and mature stages, presumably via negative selection (35, 36). Consistent with this interpretation, previous work suggests that λ-light chain expression is enriched on antigen receptors exhibiting autoreactivity (37). As anticipated, the κ:λ ratio was increased in the FM versus transitional B cell pool. However, when we compared GFP$^+$ versus GFP$^-$ CD21^{int} T2 B cells, we observed the opposite result with a significant decrease in this ratio in the more active GFP$^-$ CD21^{int} T2 subset (Fig. 10 A). Notably, compared with FM B cells, the κ:λ ratio was also lower within the T2-MZP/MZ compartment and consistent with previous reports of selection for self-reactive cells within the MZ B cell compartment.

To further investigate the apparent skewing of the BCR repertoire in the CD21^{int} T2 compartment, we used transgenic mice expressing the antiphosphorylcholine (anti-PC) M167 V_h1 heavy chain (38). In this strain, B cells expressing the PC-binding $V_h1/V_κ24$ heavy/light chain pair are nearly undetectable within the BM. In contrast, Id-specific cells are significantly enriched within the MZ compartment, most likely through antigen-driven expansion (14, 38). To determine the point in B cell development at which enrichment for PC-binding, $V_h1/V_κ24$-expressing cells is first apparent, we stained peripheral B cell subsets with anti-Id antibodies. We observed a significant increase in Id-specific, CD21^{int} T2 B cells compared with T1 cells (5–10% vs. <1%; Fig. 10, B and C). Id-specific cells were further enriched within the MZ B cell population (15–20%), whereas the FM subset exhibited little change relative to T1 B cells. Although Id-specific CD21^{int} T2 B cells were phenotypically indistinguishable from non–Id-specific cells (unpublished data), a much greater percentage of Id-specific cells had progressed beyond G0 (Fig. 10 D). Together, these data strongly suggest that low-affinity self-antigen stimulation can promote the expansion of antigen-specific CD21^{int} T2 B cells, and functions in concert with other environmental cues to facilitate recruitment into the MZ compartment.

DISCUSSION

Although microenvironmental-mediated selection is clearly operative within the transitional B cell compartment, the precise subsets that serve as targets for selection remain incompletely defined and are the subject of continued controversy. Herein, we define a transitional population that, in contrast to T1 B cells, exhibits augmented responses to a range of potential microenvironmental stimuli and shows evidence of antigen-driven expansion.

CD21^{int} T2 B cells can be distinguished both functionally and phenotypically from other splenic B cell developmental populations. High expression of GFP (in Rag2p-GFP transgenic mice) definitively establishes CD21^{int} T2 B cells as an immature transitional population. However, in contrast to early transitional B cells, these cells are larger, express higher levels of IgD and CD62L, and exhibit a significantly blunted apoptotic response after BCR engagement. CD21^{int} T2 B cells display a rapid proliferative response to LPS stimulation that, among splenic B cell subsets, is characteristic of cells committed to the MZ B cell lineage. Low expression of the Notch target genes, however, definitively distinguishes these cells from the T2-MZP developmental subset. CD21^{int} T2 B cells cycle in vivo, and the actively cycling pool exhibits further augmentation in the capacity to respond to BCR engagement and/or costimulatory signals. Cycling CD21^{int} T2 B cells express the highest levels of BAFF-R among all peripheral B cell

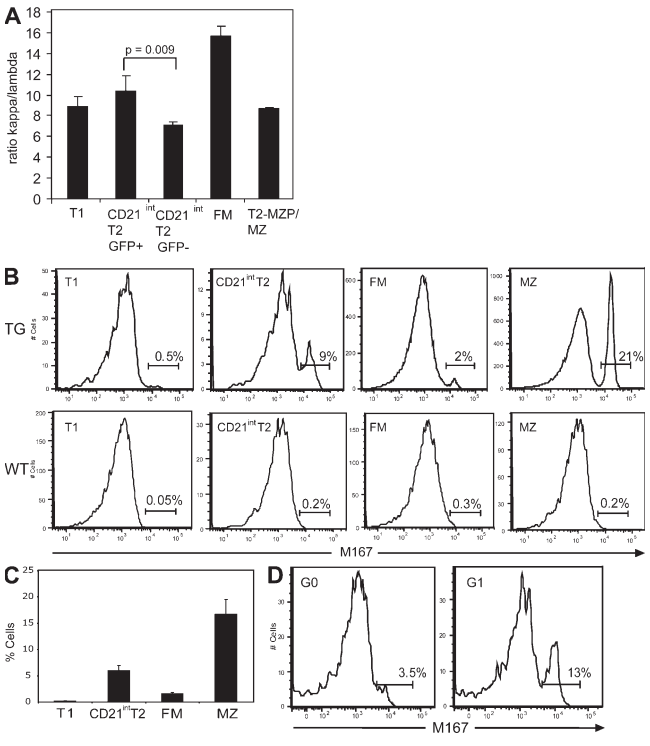

Figure 10. CD21^{int} T2 cells show evidence of antigen-mediated selection. (A) BCR κ^+/λ^+ ratio. The percentage of κ^+ versus λ^+ B cells within each B cell subset in wt mice was determined by FACS and displayed as the ratio of κ^+/λ^+ B cells. Mean of four mice with SD is shown. (B and C) Determination of percentage of Id-specific cells within each B cell subset in M167 transgenic mice. (B) Representative histograms from one M167 transgenic and wt animal. (C) Average of Id-specific cells with SD from four mice in two independent experiments. (D) Cell cycle status of Id-specific cells. Total splenocytes were stained as in Fig. 5 A, with the addition of the anti-Id antibody. Shown is the percentage of Id-specific cells in G0 or G1 within the CD21^{int} T2 population.

subsets, and BAFF mediates HP of this subset in vivo. Cycling CD21^{int} T2 B cells are partially enriched for λ^+ cells, and M167 BCR Id-specific B cells are first selected within the cycling CD21^{int} T2 population, suggesting that specific BCR ligands may promote amplification of this subpopulation.

The observation that B cells enter the periphery as immature B cells arising from the BM was first published by Allman et al. (39, 40). The term transitional B cell was subsequently introduced by Carsetti et al. describing recently migrated immature splenic B cells in transition from the immature to the mature B cell compartments and a target of BCR-mediated selection (41). Although alternative criteria have been proposed (20, 42), the Loder (19) and Allman (23) schema are now widely used by a range of investigators to characterize splenic transitional B cells in various experimental contexts anticipated to impact peripheral B cell function. However, although these schemas use a similar nomenclature, they refer to discordant late transitional B cell populations (43) and, to a large degree, have implicated alternative events in shaping the mature B cell repertoire.

Loder et al. initially defined splenic CD21^{lo}IgM^{hi}IgD^{lo}-CD24^{hi} T1 B cells as the key target for negative selection. Cells that survived this checkpoint became CD21$^{int/hi}$IgM^{hi} IgD^{hi}CD24^{hi} T2 B cells, and the authors proposed that an antigen-driven selection was required for the subsequent development of this population into either mature naive FM or MZ B cells (19).

In contrast to the aforementioned model, Allman et al. described an alternative developmental schema in which three nonproliferative transitional subsets (termed T1-T3) were identified based on relative expression of the cell surface markers AA4.1, CD23, and IgM. These developmental subsets exhibited a rapid cell turnover rate (which is consistent with a transitional stage) and no capacity to enter into the cell cycle upon BCR stimulation, but they exhibited a progressive increase in their responsiveness to CD40 and TLR stimulation (23, 42, 44).

Subsequent studies have only partially resolved the differences within these developmental models. It is now clear that the CD24^{hi}CD21$^{int/hi}$ late transitional population described by Loder et al. is both functionally and developmentally heterogeneous (19). Mice lacking expression of the NFκB p50 subunit or the Notch2 receptor exhibit a selective loss of both MZ B cells and CD24^{hi}CD21^{hi} splenic B cells (21, 45). Based on these findings, Pillai et al. suggested that the CD-24^{hi}CD21^{hi} T2 population is predominantly comprised of MZ-restricted progenitors (46). Consistent with this suggestion, Srivastava et al. showed that CD21^{hi} T2 cells comprise a long-lived, self-renewing compartment, and that development of FM B cells in sublethally irradiated animals precedes generation of this subset (22).

In contrast to CD21^{hi} T2 cells, the CD21^{int} T2 subset, as experimentally defined here, comprises a bipotent transitional population. Kinetic analysis of the peripheral B cell compartment after sublethal irradiation or after adoptive transfer of T1 cells into adult recipients demonstrates that CD21^{int} T2 cells are most likely derived from less mature splenic T1 (CD24^{hi}CD21^{lo}) progenitors. However, it might be possible that some splenic CD21^{int} T2 cells derive from early transitional cells in the BM, as two recent publications have shown that transitional cells can also develop in the BM and exit into the periphery (36, 47). Independent of where this development occurs, analysis of GFP expression (in Rag2p-GFP Tg mice) indicates that CD21^{int} B cells are newly derived (within 2–4 d, based on the half-life of GFP) from BM precursor B cells, and, in contrast to CD21^{hi} T2-MZP subset, do not comprise a long-lived population. In addition, the Notch pathway is minimally active in CD21^{int} T2 cells, and it is subsequently up-regulated in T2-MZP and MZ B cells. Finally, using adoptive transfer experiments in normal and lymphopenic recipients, we clearly show that CD21^{int} T2 B cells include the immediate precursors for both FM and MZ B cells.

Our findings also firmly establish that environmental cues can promote the proliferation of a subpopulation of cells within the CD21^{int} T2 B cell compartment. The question as to whether transitional B cells cycle has been a subject of controversy.

T2 B cells were originally described as being comprised of a large percentage of cycling cells (19). This view is supported by a recent study indicating that ~8% of $B220^+AA4.1^+CD24^{hi}$ B cells are in the S/G2 phase (48), and by studies demonstrating a proportion of Ki-67^+ cells within the transitional B cell compartment in human peripheral blood (49). In contrast, Allman et al. have consistently reported that transitional B cells do not contain significant numbers of cycling cells (22, 23), and this conclusion has been supported by others using similar gating criteria (44). We used several alternative approaches to determine whether $CD21^{int}$ T2 B cells are cycling within the spleen, including DAPI/Pyronin Y staining, measurement of KRECs in splenic B cell subsets, and short-term in vivo BrdU-labeling kinetics. Our combined data from these analyses clearly indicate that a small but consistent fraction of $CD21^{int}$ T2 B cells is cycling in vivo.

Differences between our data and previously published cell cycle analyses may be caused, in part, by alternative cell gating strategies. Using the Allman transitional B cell gating schema and seven-color flow cytometry, cycling $CD21^{int}$ T2 cells fall within each of the T1–T3 subsets, and because of the relatively small size of this population they are nearly undetectable (Fig. S6, available at http://www.jem.org/cgi/content/full/jem.20071088/DC1). In contrast, gating as shown in Fig. 1 readily identifies cycling cells. This latter observation additionally strengthens our interpretation that $CD21^{int}$ T2 B cells comprise a distinct, late transitional subset.

Our observations partially define the signals that mediate cycling within the late transitional B cell compartment. When transferred into a B cell–sufficient host, $CD21^{int}$ T2 B cells proliferate very little, although they develop into both FM and T2-MZP/MZ B cells, indicating that cycling is not a prerequisite for entering the mature B cell pool. In contrast, as shown here and as previously described (30, 50), both mature and transitional B cells proliferate when introduced into a lymphopenic environment, a process termed HP. Because B cell deficiency leads to increased levels of BAFF in both humans and mice (18, 51), we hypothesized that BAFF signals are involved in HP. Although B cells do not proliferate in response to BAFF in vitro, BAFF can induce entry into early G1 (52). Moreover, stimulation with BAFF leads to an increase in cell size and glucose metabolism (31), up-regulation of Ki-67, Cyclin D2, and Cdk4 expression, and phosphorylation of RB and Akt (53). These findings, combined with our experimental data, strongly suggest that in vivo, BAFF is critical for cycling of $CD21^{int}$ T2 B cells. Consistent with this model, inhibition of BAFF markedly attenuated the cycling of $CD21^{int}$ T2 cells in μMT hosts, and $CD21^{int}$ T2 B cells in G1 and beyond expressed the highest levels of BAFF-R, findings that directly correlated with preferential proliferative responses in lymphopenic hosts.

There is mounting evidence that alterations in transitional B cell homeostasis mediated by BAFF can significantly impact the mature BCR repertoire (30, 32, 54). Under normal physiological conditions, B cells directly compete for available BAFF (18, 54), autoreactive B cells can be rescued by strong BAFF signals (17, 18), and data from both humans and mice indicate that these selective forces operate at the transitional stage (6, 54). Whether autoreactive B cells can be specifically expanded within the transitional B cell pool, however, represents a crucial unanswered question. Using the M167 BCR heavy chain transgenic mouse, we observed a marked expansion of PC-binding B cells within the $CD21^{int}$ T2 compartment. Further, our data demonstrate that this Id-specific $CD21^{int}$ T2 B cell population is significantly enriched for cycling cells. In addition, we also identified a clear increase in the relative percentage of λ^+ cells specifically within the cycling $CD21^{int}$ T2 B cell population. This enrichment contrasts with the progressive decline in λ^+ cells observed across other sequential peripheral B cell subsets, as shown here and as previously described (36). Collectively, these observations strongly imply that cells expressing a self-reactive BCR can be specifically amplified with the $CD21^{int}$ T2 B cell subset.

Although proliferation or antigen-driven expansion of $CD21^{int}$ T2 cells is clearly not required for the generation of mature B cells, our combined data support a model in which antigen encounter (in concert with environmental cues including BAFF) can promote the competitive expansion of cells within this compartment. According to the measurement of KRECs, $CD21^{int}$ T2 cells and T2-MZP/MZ cells have undergone a similar number of cell divisions. However, our BrdU studies suggest that this cell division occurs preferentially at the $CD21^{int}$ T2 stage. These combined findings imply that $CD21^{int}$ T2 cells, upon receiving the appropriate signals, begin to divide and are preferentially driven into a MZ B cell fate. Because BCR engagement positively modulates BAFF-R expression (16), our findings also suggest that BCR signaling coordinately amplifies BAFF-independent and -dependent signals within the cycling $CD21^{int}$ T2 subpopulation. This selection program appears to be enhanced in conditions leading to high BAFF levels, as experimentally implied in our adoptive transfer and BAFF inhibition experiments. Accordingly, in BAFF transgenic mice, autoreactive cells are primarily found within the MZ (48) and high BAFF levels in humans promote autoimmune diseases, including Sjogren's syndrome (55).

Finally, in light of the developmental capacity of the $CD21^{int}$ T2 B cell subset, it remains possible that antigen-expanded cells might also develop into FM B cells. Although it is not addressed in this study, such a scenario might be operative in selected autoimmune-prone genetic contexts. Identification of a transitional population where self-reactive B cells are initially expanded sets the stage for a range of future studies investigating the selective forces operative at this key point in peripheral B cell development.

MATERIALS AND METHODS

Mice. BALB/c, C57BL/6 (Ly5.1 and Ly5.2), μMT, and Rag2p-GFP mice were bred and maintained in the specific pathogen–free animal facility of the Children's Hospital and Regional Medical Center (Seattle, WA) and handled according to Institutional Animal Care and Use Committee approved protocols. Notch2 haplodeficient mice were provided by T. Gridley

(Jackson ImmunoResearch Laboratories). M167 heavy chain transgenic mice (M167H Tg mice, line U243-4) were provided by J. Kenny and A. Lustig (National Institute of Aging, Bethesda, MD) and established as a M167H Tg/Tg homozygous breeding colony in the animal facility of the Albert Einstein College of Medicine. Mice used in all experiments were between 6 and 16 wk of age.

Reagents and antibodies. Antibodies used in this study included reagents specific for the following: active-caspase 3 (C92-605), CD24 (M1/69), CD21 (7G6), B220 (RA3-6B2), and CD1d (1B1; BD Biosciences); CD23 (B3B4; Invitrogen); Ly5.1 (A20), Ly5.2 (RA3-6B2), AA4.1, and CD62L (MEL-14; eBioscience); IgD (11-26), κ-LC (187.1), λ-LC (JC5-1), and IgM (1B4B1; SouthernBiotech); CD19 (ID3; BioLegend); and BAFF-R (204406; R&D Systems). Polyclonal $F(ab')_2$ anti-IgM for BCR stimulation and non-stimulatory Fab anti-IgM for cell sorting were purchased from Jackson ImmunoResearch Laboratories. Antiidiotypic M167 (28-5-15) was produced from a hybridoma line provided by J. Kenny and A. Lustig, and it was purified and conjugated with Alexa Fluor 647 using standard methods. Additional reagents included the following: 7-amino actinomycin D (7-AAD), Pyronin Y, and DAPI (Invitrogen); LPS (Sigma-Aldrich); anti-CD40 (a gift from G. Cheng, University of California Los Angeles, Los Angeles, CA); and recombinant mouse BAFF (Thermo Fisher Scientific).

Flow cytometry and cell sorting. Single-cell suspensions from BM and spleen were incubated with fluorescently labeled antibodies for 30 min at 4°C in staining buffer (PBS with 0.5% BSA or 2.5% FCS). Data were collected on a FACSCalibur or LSR II flow cytometer (BD Biosciences) and analyzed using FlowJo software (Tree Star, Inc.). Overlays of histogram are shown using the offset mode in FlowJo. For LSR II experiments, the data were analyzed using biexponential transformation function for complete data visualization. For caspase 3 assays, cells were surface stained, fixed, and permeabilized per manufacturer's instructions, and incubated with anti–active caspase 3 for 45 min at room temperature. 7-AAD was used to differentiate between dead and live cells. For cell cycle analysis, cells were surface stained, fixed overnight with 2% PFA, washed, and incubated for 30 min with 1 μg/ml DAPI in PBS with 0.1% BSA and 0.1% Triton X-100. 1.5 μg/ml Pyronin Y was added immediately before analysis.

For cell sorting, CD43 depletion was performed using magnetic bead–conjugated anti-CD43 antibodies according to the manufacturer's instructions (Miltenyi Biotech), and enriched cells were labeled with specific antibodies in staining buffer. Sorting was performed using a FACSAria sorter with FACSDiva software (BD Biosciences).

Cell culture and proliferation assays. Purified cells were cultured in complete media (RPMI 1640 with 10% FCS, 4 μM L-glutamine, 50 μM 2-ME, 10 mM Hepes, and antibiotics) at 37°C. Cells were stimulated with 10 μg/ml polyclonal goat $F(ab')_2$ fragment anti–mouse IgM, 1 μg/ml anti–mouse CD40, 10 μg/ml LPS, or 50 ng/ml BAFF; incubated in triplicate (5×10^4 cells/well) for 48 h; pulsed with 1 μCi [^{3}H]thymidine for 8 h before harvesting, and analyzed using a scintillation counter.

Real-time PCR. Sorted B cell populations were pelleted and frozen at –80°C. RNA was isolated using the RNeasy Micro kit (QIAGEN) and converted into cDNA by reverse transcription (Superscript II; Invitrogen) according to the manufacturer's instructions. Real-time PCR on cDNA was performed using the iCycler real-time PCR detection system with IQ SYBR Green Supermix (Bio-Rad Laboratories) according to the manufacturer's instructions. Ratios were calculated using the Pfaffl's mathematical model for relative quantification (56), with mouse β2-microglobulin as housekeeping control. All real-time PCR analysis shown includes at least three independent experiments. Primer sequences used include the following: Hes1-5′GAGAAGAGGCGAAGGGCAAGAAT; Hes1-3′ GAGGTGCTTCACAGTCA; Deltex1-5′ CGGACATTTGAGACCCACTT; Deltex1-3′ CCACTTTCAAGCAGGGAGAA; CyclinD2-5′ GCCAAGATCACCCACACT; and CyclinD2-3′ GCTGCTCTTGACGGAACT. To determine the replication history of B cells, genomic DNA was isolated from sorted populations and the ratio between the κ-deleting rearrangement (IRS1 to RS) and excision circles (KREC) was determined by TaqMan-based (Applied Biosystems) real-time PCR, as previously described (28).

BrdU incorporation. Continuous in vivo BrdU labeling was performed by feeding mice BrdU via the drinking water containing 1 μg/ml BrdU (Sigma-Aldrich) and 10% sucrose. Mice were killed at indicated time points, and splenocytes were surface stained to identify splenic B cell subsets. Cells were then fixed and permeabilized, treated with DNase, and stained with anti-BrdU FITC (BrdU kit from BD Biosciences).

Adoptive cell transfer. CD43-depleted B cells or sorted B cell subsets were incubated with 0.05 μM CFSE at 37°C for 8 min, washed three times with complete media, and then washed with PBS. In experiments using "feeder" B cells, CD43-depleted splenic B cells were prepared and mixed with sorted B cells. For transfer of sorted T1 or CD21^{int} T2 B cells, a total number of 15×10^6 cells in 250 μl PBS were injected by tail vein into μMT or C57BL/6 mice.

In vivo inhibition of BAFF. TACI- or control GFP-adenovirus (provided by R. Carter, University of Alabama, Tuscaloosa, AL) were prepared as previously described (33) and injected into the tail vein at 10^9 PFU per recipient, followed 6–7 d later by transfer of 20×10^6 CD43-depleted, CFSE-labeled splenic B cells (Ly5.1$^+$). Mice were killed 5 d after adoptive transfer, and splenocytes were stained for B220, CD19, CD24, CD21, CD1d, IgM, and Ly5.1.

Online supplemental material. Fig. S1 shows sorting gates and postsort purities. Fig. S2 shows the phenotypic and functional properties of CD21^{int} T2 cells from irradiated mice. Fig. S3 shows how cell cycle subsets are gated. Fig. S4 shows surface markers on GFP$^+$ versus GFP$^-$ CD21^{int} T2 cells. Fig. S5 compares the expression of cell surface markers on B cells from control versus TACI-Ad–treated mice. Fig. S6 compares transitional subsets, as gated by Allman et al., and CD21^{int} T2 B cells. Table S1 summarizes the expression of cell surface markers on peripheral B cell subsets described in this work. The online version of this article is available at http://www.jem.org/cgi/content/full/jem.20071088/DC1.

We thank R. Carter for providing TACI-adenoviral vector; M. Nussenzweig (Rockefeller University) for Rag2p-GFP transgenic mice; J. Kenny and A. Lustig for M167H transgenic mice and hybridoma lines; and S. Khim, N. Blake, and A. Hui for expert technical assistance with animal studies, flow cytometry, and manuscript preparation, respectively.

Support for this work has included the Elizabeth Campbell Endowment (A. Meyer-Bahlburg), Cancer Research Institute immunology training grant (S.F. Andrews), the Medical Scientist Training Program at the Albert Einstein College of Medicine (K.O.A. Yu), and National Institutes of Health grants HD37091, CA81140, AI45889, and AI063537.

The authors have no conflicting financial interests.

Submitted: 30 May 2007
Accepted: 21 November 2007

REFERENCES

1. Hardy, R.R., and K. Hayakawa. 2001. B cell development pathways. *Annu. Rev. Immunol.* 19:595–621.
2. Goodnow, C.C. 1996. Balancing immunity and tolerance: deleting and tuning lymphocyte repertoires. *Proc. Natl. Acad. Sci. USA.* 93: 2264–2271.
3. Melchers, F. 2006. Anergic B cells caught in the act. *Immunity.* 25: 864–867.
4. Wardemann, H., S. Yurasov, A. Schaefer, J.W. Young, E. Meffre, and M.C. Nussenzweig. 2003. Predominant autoantibody production by early human B cell precursors. *Science.* 301:1374–1377.
5. Samuels, J., Y.S. Ng, C. Coupillaud, D. Paget, and E. Meffre. 2005. Impaired early B cell tolerance in patients with rheumatoid arthritis. *J. Exp. Med.* 201:1659–1667.

6. Yurasov, S., H. Wardemann, J. Hammersen, M. Tsuiji, E. Meffre, V. Pascual, and M.C. Nussenzweig. 2005. Defective B cell tolerance checkpoints in systemic lupus erythematosus. *J. Exp. Med.* 201:703–711.
7. Russell, D.M., Z. Dembic, G. Morahan, J.F. Miller, K. Burki, and D. Nemazee. 1991. Peripheral deletion of self-reactive B cells. *Nature.* 354:308–311.
8. Kench, J.A., D.M. Russell, and D. Nemazee. 1998. Efficient peripheral clonal elimination of B lymphocytes in MRL/lpr mice bearing autoantibody transgenes. *J. Exp. Med.* 188:909–917.
9. Levine, M.H., A.M. Haberman, D.B. Sant'Angelo, L.G. Hannum, M.P. Cancro, C.A. Janeway Jr., and M.J. Shlomchik. 2000. A B-cell receptor-specific selection step governs immature to mature B cell differentiation. *Proc. Natl. Acad. Sci. USA.* 97:2743–2748.
10. Gu, H., D. Tarlinton, W. Muller, K. Rajewsky, and I. Forster. 1991. Most peripheral B cells in mice are ligand selected. *J. Exp. Med.* 173: 1357–1371.
11. Gaudin, E., Y. Hao, M.M. Rosado, R. Chaby, R. Girard, and A.A. Freitas. 2004. Positive selection of B cells expressing low densities of self-reactive BCRs. *J. Exp. Med.* 199:843–853.
12. Cyster, J.G., J.I. Healy, K. Kishihara, T.W. Mak, M.L. Thomas, and C.C. Goodnow. 1996. Regulation of B-lymphocyte negative and positive selection by tyrosine phosphatase CD45. *Nature.* 381:325–328.
13. Wang, H., and S.H. Clarke. 2003. Evidence for a ligand-mediated positive selection signal in differentiation to a mature B cell. *J. Immunol.* 171:6381–6388.
14. Balazs, M., F. Martin, T. Zhou, and J. Kearney. 2002. Blood dendritic cells interact with splenic marginal zone B cells to initiate T-independent immune responses. *Immunity.* 17:341–352.
15. Schiemann, B., J.L. Gommerman, K. Vora, T.G. Cachero, S. Shulga-Morskaya, M. Dobles, E. Frew, and M.L. Scott. 2001. An essential role for BAFF in the normal development of B cells through a BCMA-independent pathway. *Science.* 293:2111–2114.
16. Smith, S.H., and M.P. Cancro. 2003. Cutting edge: B cell receptor signals regulate BLyS receptor levels in mature B cells and their immediate progenitors. *J. Immunol.* 170:5820–5823.
17. Thien, M., T.G. Phan, S. Gardam, M. Amesbury, A. Basten, F. Mackay, and R. Brink. 2004. Excess BAFF rescues self-reactive B cells from peripheral deletion and allows them to enter forbidden follicular and marginal zone niches. *Immunity.* 20:785–798.
18. Lesley, R., Y. Xu, S.L. Kalled, D.M. Hess, S.R. Schwab, H.B. Shu, and J.G. Cyster. 2004. Reduced competitiveness of autoantigen-engaged B cells due to increased dependence on BAFF. *Immunity.* 20:441–453.
19. Loder, F., B. Mutschler, R.J. Ray, C.J. Paige, P. Sideras, R. Torres, M.C. Lamers, and R. Carsetti. 1999. B cell development in the spleen takes place in discrete steps and is determined by the quality of B cell receptor-derived signals. *J. Exp. Med.* 190:75–89.
20. Pillai, S., A. Cariappa, and S.T. Moran. 2005. Marginal zone B cells. *Annu. Rev. Immunol.* 23:161–196.
21. Saito, T., S. Chiba, M. Ichikawa, A. Kunisato, T. Asai, K. Shimizu, T. Yamaguchi, G. Yamamoto, S. Seo, K. Kumano, et al. 2003. Notch2 is preferentially expressed in mature B cells and indispensable for marginal zone B lineage development. *Immunity.* 18:675–685.
22. Srivastava, B., W.J. Quinn III, K. Hazard, J. Erikson, and D. Allman. 2005. Characterization of marginal zone B cell precursors. *J. Exp. Med.* 202:1225–1234.
23. Allman, D., R.C. Lindsley, W. DeMuth, K. Rudd, S.A. Shinton, and R.R. Hardy. 2001. Resolution of three nonproliferative immature splenic B cell subsets reveals multiple selection points during peripheral B cell maturation. *J. Immunol.* 167:6834–6840.
24. Yu, W., H. Nagaoka, M. Jankovic, Z. Misulovin, H. Suh, A. Rolink, F. Melchers, E. Meffre, and M.C. Nussenzweig. 1999. Continued RAG expression in late stages of B cell development and no apparent re-induction after immunization. *Nature.* 400:682–687.
25. Nagaoka, H., G. Gonzalez-Aseguinolaza, M. Tsuji, and M.C. Nussenzweig. 2000. Immunization and infection change the number of recombination activating gene (RAG)-expressing B cells in the periphery by altering immature lymphocyte production. *J. Exp. Med.* 191:2113–2120.
26. Schmid, I., S.W. Cole, Y.D. Korin, J.A. Zack, and J.V. Giorgi. 2000. Detection of cell cycle subcompartments by flow cytometric estimation of DNA-RNA content in combination with dual-color immunofluorescence. *Cytometry.* 39:108–116.
27. Su, T.T., and D.J. Rawlings. 2002. Transitional B lymphocyte subsets operate as distinct checkpoints in murine splenic B cell development. *J. Immunol.* 168:2101–2110.
28. van Zelm, M.C., T. Szczepanski, M. van der Burg, and J.J. van Dongen. 2007. Replication history of B lymphocytes reveals homeostatic proliferation and extensive antigen-induced B cell expansion. *J. Exp. Med.* 204:645–655.
29. Singh, N.J., and R.H. Schwartz. 2006. The lymphopenic mouse in immunology: from patron to pariah. *Immunity.* 25:851–855.
30. Woodland, R.T., and M.R. Schmidt. 2005. Homeostatic proliferation of B cells. *Semin. Immunol.* 17:209–217.
31. Woodland, R.T., M.R. Schmidt, and C.B. Thompson. 2006. BLyS and B cell homeostasis. *Semin. Immunol.* 18:318–326.
32. Cancro, M.P. 2004. The BLyS family of ligands and receptors: an archetype for niche-specific homeostatic regulation. *Immunol. Rev.* 202:237–249.
33. Liu, W., A. Szalai, L. Zhao, D. Liu, F. Martin, R.P. Kimberly, T. Zhou, and R.H. Carter. 2004. Control of spontaneous B lymphocyte autoimmunity with adenovirus-encoded soluble TACI. *Arthritis Rheum.* 50:1884–1896.
34. Gorelik, L., A.H. Cutler, G. Thill, S.D. Miklasz, D.E. Shea, C. Ambrose, S.A. Bixler, L. Su, M.L. Scott, and S.L. Kalled. 2004. Cutting edge: BAFF regulates CD21/35 and CD23 expression independent of its B cell survival function. *J. Immunol.* 172:762–766.
35. Dingjan, G.M., S. Middendorp, K. Dahlenborg, A. Maas, F. Grosveld, and R.W. Hendriks. 2001. Bruton's tyrosine kinase regulates the activation of gene rearrangements at the lambda light chain locus in precursor B cells in the mouse. *J. Exp. Med.* 193:1169–1178.
36. Lindsley, R.C., M. Thomas, B. Srivastava, and D. Allman. 2006. Generation of peripheral B cells occurs via two spatially and temporally distinct pathways. *Blood.* 109:2521–2528.
37. Doyle, C.M., J. Han, M.G. Weigert, and E.T. Prak. 2006. Consequences of receptor editing at the lambda locus: multireactivity and light chain secretion. *Proc. Natl. Acad. Sci. USA.* 103:11264–11269.
38. Kenny, J.J., C. O'Connell, D.G. Sieckmann, R.T. Fischer, and D.L. Longo. 1991. Selection of antigen-specific, idiotype-positive B cells in transgenic mice expressing a rearranged M167-mu heavy chain gene. *J. Exp. Med.* 174:1189–1201.
39. Allman, D.M., S.E. Ferguson, and M.P. Cancro. 1992. Peripheral B cell maturation. I. Immature peripheral B cells in adults are heat-stable antigenhi and exhibit unique signaling characteristics. *J. Immunol.* 149: 2533–2540.
40. Allman, D.M., S.E. Ferguson, V.M. Lentz, and M.P. Cancro. 1993. Peripheral B cell maturation. II. Heat-stable antigen(hi) splenic B cells are an immature developmental intermediate in the production of long-lived marrow-derived B cells. *J. Immunol.* 151:4431–4444.
41. Carsetti, R., G. Kohler, and M.C. Lamers. 1995. Transitional B cells are the target of negative selection in the B cell compartment. *J. Exp. Med.* 181:2129–2140.
42. Chung, J.B., R.A. Sater, M.L. Fields, J. Erikson, and J.G. Monroe. 2002. CD23 defines two distinct subsets of immature B cells which differ in their responses to T cell help signals. *Int. Immunol.* 14:157–166.
43. Chung, J.B., M. Silverman, and J.G. Monroe. 2003. Transitional B cells: step by step towards immune competence. *Trends Immunol.* 24:343–349.
44. Hsu, B.L., S.M. Harless, R.C. Lindsley, D.M. Hilbert, and M.P. Cancro. 2002. Cutting edge: BLyS enables survival of transitional and mature B cells through distinct mediators. *J. Immunol.* 168:5993–5996.
45. Cariappa, A., H.C. Liou, B.H. Horwitz, and S. Pillai. 2000. Nuclear factor kappa B is required for the development of marginal zone B lymphocytes. *J. Exp. Med.* 192:1175–1182.
46. Pillai, S., A. Cariappa, and S.T. Moran. 2004. Positive selection and lineage commitment during peripheral B-lymphocyte development. *Immunol. Rev.* 197:206–218.

47. Cariappa, A., C. Chase, H. Liu, P. Russell, and S. Pillai. 2006. Naive recirculating B cells mature simultaneously in the spleen and bone marrow. *Blood*. 109:2339–2345.
48. Enzler, T., G. Bonizzi, G.J. Silverman, D.C. Otero, G.F. Widhopf, A. Anzelon-Mills, R.C. Rickert, and M. Karin. 2006. Alternative and classical NF-kappa B signaling retain autoreactive B cells in the splenic marginal zone and result in lupus-like disease. *Immunity*. 25:403–415.
49. Wirths, S., and A. Lanzavecchia. 2005. ABCB1 transporter discriminates human resting naive B cells from cycling transitional and memory B cells. *Eur. J. Immunol.* 35:3433–3441.
50. Cabatingan, M.S., M.R. Schmidt, R. Sen, and R.T. Woodland. 2002. Naive B lymphocytes undergo homeostatic proliferation in response to B cell deficit. *J. Immunol.* 169:6795–6805.
51. Lavie, F., C. Miceli-Richard, M. Ittah, J. Sellam, J.E. Gottenberg, and X. Mariette. 2006. Increase of B-cell activating factor of the TNF family (BAFF) after rituximab: insights into a new regulating system of BAFF production. *Ann Rheum Dis*. 202:496–502.
52. Huang, X., M. Di Liberto, A.F. Cunningham, L. Kang, S. Cheng, S. Ely, H.C. Liou, I.C. Maclennan, and S. Chen-Kiang. 2004. Homeostatic cell-cycle control by BLyS: Induction of cell-cycle entry but not G1/S transition in opposition to p18INK4c and p27Kip1. *Proc. Natl. Acad. Sci. USA*. 101:17789–17794.
53. Patke, A., I. Mecklenbrauker, H. Erdjument-Bromage, P. Tempst, and A. Tarakhovsky. 2006. BAFF controls B cell metabolic fitness through a PKC beta- and Akt-dependent mechanism. *J. Exp. Med*. 203: 2551–2562.
54. Brink, R. 2006. Regulation of B cell self-tolerance by BAFF. *Semin. Immunol.* 18:276–283.
55. Groom, J., S.L. Kalled, A.H. Cutler, C. Olson, S.A. Woodcock, P. Schneider, J. Tschopp, T.G. Cachero, M. Batten, J. Wheway, et al. 2002. Association of BAFF/BLyS overexpression and altered B cell differentiation with Sjogren's syndrome. *J. Clin. Invest*. 109:59–68.
56. Pfaffl, M.W. 2001. A new mathematical model for relative quantification in real-time RT-PCR. *Nucleic Acids Res*. 29:e45.